Modeling enhancement and suppression of vibrational Feshbach resonances in positron annihilation on molecules

J. R. Danielson, A. C. L. Jones, M. R. Natisin, and C. M. Surko*
9500 Gilman Drive, Physics Department, University of California, San Diego, La Jolla, California 92093, USA
(Received 5 September 2013; published 4 December 2013)

Experiments have shown that positrons can attach to molecules via vibrational Feshbach resonances. This leads to increased annihilation rates, the magnitudes of which depend upon molecular structure. Presented here is a simplified rate-equation model to describe the competition between annihilation while the positron is attached to the molecule, positron ejection from the entrance state, and diffusion of the vibrational energy to multimode states followed by similar ejection due to vibrational deexcitation. The latter ejection process can involve vibrations more strongly coupled to the positron continuum, producing suppression of the annihilation, or those more weakly coupled to the continuum, resulting in enhanced annihilation rates. This model elucidates the role that mode coupling can play in determining resonant annihilation amplitudes. Simple limits are obtained and compared with experimental results for selected molecules.

DOI: 10.1103/PhysRevA.88.062702 PACS number(s): 34.80.Uv, 33.15.Hp, 34.80.Lx, 34.50.Ez

I. INTRODUCTION

While positron interactions with ordinary matter are important in a variety of contexts including materials science, medicine, and astrophysics [1–3], many fundamental processes remain to be understood. The focus here is one such process, namely, positron annihilation on molecules. It has been shown experimentally that positrons bind to most polyatomic molecules [4–6]. While less mature than the experimental studies, theories are now also available to predict positron binding energies for selected small molecules [7–9].

Attachment occurs in positron-molecule collisions via excitation of a vibrational Feshbach resonance (VFR) involving the excitation of one or more vibrational modes. The resulting positron-molecule complex is not a true bound state but a resonance, because there is still sufficient vibrational energy to eject the positron. As a result, the positron can subsequently be ejected from the molecule by the deexcitation of a vibrational mode or modes. However, while attached, the annihilation rate is enhanced greatly as compared to that for a simple collision. All positrons that remain on the molecule will annihilate if the dwell time is $\gtrsim$1–10 ns.

Annihilation rates are typically expressed in terms of the dimensionless quantity $Z_{\rm eff}$, which is obtained by normalizing the measured annihilation rate λ by the Dirac annihilation rate Γ^D for a free-electron gas of the same number density n_m [4],

$$Z_{\rm eff} \equiv \frac{\lambda}{\Gamma^D} = \frac{\lambda}{\pi r_0^2 c n_m}, \tag{1}$$

where c is the speed of light and r_0 is the classical electron radius. Feshbach resonances typically occur at incident positron energies ε_ν such that

$$\varepsilon_\nu = \omega_\nu - \varepsilon_b, \tag{2}$$

where ε_b is the positron binding energy and ω_ν is the energy of fundamental vibration ν. The relative positions of the various resonances observed in a particular molecule are consistent to within a few millielectronvolts with those predicted by Eq. (2), thus providing evidence that the measured binding energies ε_b are insensitive to the vibrational motion of the molecule, and hence they characterize the true bound states.

A simple theory of resonant annihilation due to isolated VFRs is successful in predicting $Z_{\rm eff}$ as a function of incident positron energy for small molecules such as methyl halides [10]. However, this theory is inadequate to explain many annihilation features in a range of molecules, including, for example, large enhancements of resonances in alkanes and the suppression of resonances in hydrocarbons in which a hydrogen atom is replaced by a fluorine [4]. The working hypothesis is that IVR (i.e., intramolecular vibrational energy redistribution) is involved, whereby the initially excited vibration transfers its energy to other vibrations coupled more weakly to the positron continuum (leading to enhanced resonant amplitudes) or more strongly to the continuum (thus suppressing the resonance) [4].

An open question is how these ideas can be made more precise. Recently, we were able to trace the origin of the enhancement and suppression of annihilation resonances in selected molecules, such as chloroform, chloroform-d, and acetaldehyde, to specific combinations of multimodes and their coupling to the positron continuum relative to that of the initially resonant fundamental [11]. Continuing this theme, presented here is a simplified rate-equation model that further elucidates the effect that coupling to multimode vibrations can have on the amplitudes of the annihilation resonances. The model attempts to describe the competition between attachment, annihilation on the molecule, and ejection from it by coupling a resonant mode to (for simplicity) a restricted set of multimode states. Normalized annihilation rates are given for simple limiting cases, and where possible, these predictions are compared with selected observations. Additional considerations and further refinements are also discussed.

II. THE ROLE OF IVR IN RESONANT ANNIHILATION

A. Model of enhancement and suppression due to mode coupling

As discussed above, if a molecule can bind a positron, an incident positron with energy ε_ν, given by Eq. (2), can

*csurko@physics.ucsd.edu

excite mode ν to become trapped on the molecule via a vibrational Feshbach resonance. For a positron at the resonant energy, the capture rate is proportional to the elastic rate Γ^e_ν for positron ejection from the molecule by deexcitation of mode ν [4,10]. The trapped positron can then be either ejected by this process (deexcitation of mode ν) or annihilate with a molecular electron. Denoting Γ^a as the rate of annihilation in the attached state, the competition between these processes yields a dependence of the resonant contribution to $Z_{\rm eff}$ on Γ^a and Γ^e_ν of the form

$$Z_{\rm eff} \propto \Gamma^a \left(\frac{\Gamma^e_\nu}{\Gamma^a + \Gamma^e_\nu} \right). \tag{3}$$

If $\Gamma^e_\nu \gg \Gamma^a$, all resonances have similar strengths, with $Z_{\rm eff} \propto \Gamma^a$.

Considered here is the important practical situation, occurring in all but the smallest polyatomics, in which mode ν is coupled resonantly to multimode vibrations (i.e., combinations or overtones involving lower-energy fundamental modes) at a rate comparable to or greater than Γ^e_ν. In other words, the primary, single-mode resonance ν plays the role of an entrance channel that, in turn, can couple to multimode vibrational states [12]. In this case, the second factor in Eq. (3) can be modified significantly. If the vibrational energy diffuses to modes weakly coupled to the positron continuum by this process, the dwell time of the positron on the molecule will be lengthened and $Z_{\rm eff}$ will be enhanced. In contrast, if the multimode vibration contains fundamental vibrations ν strongly coupled to the positron continuum, and if $\omega_\nu > \varepsilon_b$, the positron can be rapidly ejected, leading to a decrease in $Z_{\rm eff}$.

The model of this process, which is the focus of this paper, is illustrated schematically in Fig. 1. A single entrance-channel, fundamental vibration $|\nu\rangle$ is coupled to a set of M multimode vibrations (labeled $|x\rangle$) at mode coupling rate γ. For simplicity, the M multimodes $|x\rangle$ are assumed to be identical. The positron is initially captured into state $|\nu\rangle$ at a capture rate Γ^c (specified below) which is proportional to Γ^e_ν but also includes dependence on molecular density and the energy spread of

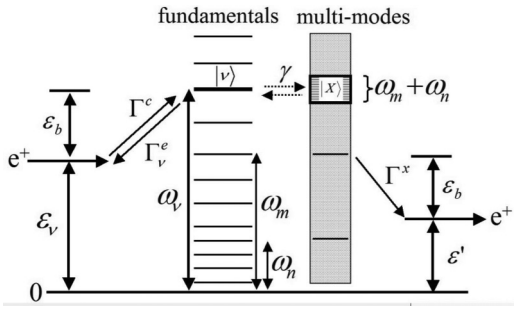

FIG. 1. Schematic diagram of the model. An incident positron is captured via a VFR into an entrance vibrational state $|\nu\rangle$ (with energy ω_ν) couples at rate γ to a set of M identical multimodes $|x\rangle$. Illustrated is $|x\rangle$ as the two-mode combination, $\omega_m + \omega_n$. If ω_m deexcites, for example, and $\omega_m \geqslant \varepsilon_b$, the positron can be ejected with energy $\varepsilon' = \omega_m - \varepsilon_b$, leaving the molecule with vibrational energy ω_n. If the escape rate Γ^x is large (small) compared to the elastic rate Γ^e_ν, the dwell time on the molecule will be shorter (longer) and the annihilation rate will be decreased (increased).

the incident positrons. The coupling rate of mode $|\nu\rangle$ to the positron continuum is Γ^e_ν.

The model assumes that the multimodes $|x\rangle$ are coupled to the positron continuum at a rate Γ^x that includes partial deexcitations of vibrations $|x\rangle$ with sufficient energy to eject the attached positron, namely,

$$\Gamma^x = \sum_j \Gamma^e_j, \tag{4}$$

where Γ^e_j is the elastic escape rate from the state j, and the sum on j includes all fundamental vibrations in multimode $|x\rangle$ for which $\omega_j \geqslant \varepsilon_b$. Multiple deexcitations of fundamentals in $|x\rangle$ are neglected as higher-order processes. These multimode states $|x\rangle$ were considered previously in describing broad backgrounds observed in resonant annihilation spectra (i.e., spectral features termed statistical multimode resonant annihilation, SMRA) [13].

The model is highly idealized in the sense that it treats all modes $|x\rangle$ as identical, whereas it is known that, in many cases, IVR proceeds through a tiered coupling from one mode to combination and overtones involving two modes, then to three-mode combinations, etc. [14,15]. The truncation assumed here is pragmatic and motivated by the fact that consideration of additional processes would introduce more parameters; at present, we do not have the ability to even approximate more than a few parameters, such as γ, Γ^e_ν, Γ^x, and M. Direct excitation of these multimodes is neglected in the model.

The number of multimodes M is introduced to keep the model simple enough to make predictions that can be interpreted relatively easily. If a molecule has a combination of many gray states (i.e., states that couple only weakly to the positron continuum) and a few fast escape channels, then the assumption that all multimodes have similar γ and act similarly is invalid. If, on the other hand, one type of mode dominates, then treating them as a group is plausible, and the predictions of the model can provide insight into the relevant physical process. As discussed below, in comparing the model to experimental data for specific VFR, fundamental modes are chosen for which the assumptions of the model appear to be reasonable, namely, that the M multimodes couple similarly to the fundamental and to the positron continuum and hence can be considered as a group.

The mode coupling parameters γ describe the coupling between fundamental modes and near-resonant multimodes. While, in principle, they could be calculated theoretically, they are not generally available for the molecules of interest. This is a major source of uncertainty, and so, in the comparisons below, limits are explored that are insensitive to the value of this parameter.

Assuming dipole coupling of the positron to infrared active modes, the rate Γ^e_ν for mode ν is given by [10]

$$\Gamma^e_\nu = \frac{16\omega_\nu d_\nu^2}{27\hbar e^2 a_0^2} h(\zeta), \tag{5}$$

where d_ν is the transition dipole matrix element in units of Coulomb-meters, a_0 is the Bohr radius, and $h(\zeta)$ is a dimensionless function of $\zeta = 1 - \varepsilon_b/\varepsilon_\nu$ [10]. Positrons annihilate in all vibrational states at the same rate Γ^a, which can be

written [4]

$$\Gamma^a = \pi r_0^2 c F \frac{\kappa}{2\pi}, \tag{6}$$

where $F = 0.66/{a_0}^2$ describes the electron-positron overlap, and $\kappa = (2m\varepsilon_b)^{1/2}/\hbar$.

The measured annihilation rate will be the probability that the positron is attached to the molecule in either state $|\nu\rangle$ or states $|x\rangle$, multiplied by the annihilation rate in the attached state, Γ^a. The quantity P^ν is defined as the probability that the positron is attached to the molecule with mode $|\nu\rangle$ excited, and P^x denotes the probability that the positron is attached to the molecule with a multimode state $|x\rangle$ excited. The effects of finite temperature are neglected. In this notation, the rate equations for P^ν and P^x are

$$\frac{dP^\nu}{dt} = \Gamma^c + M\gamma P^x - \Gamma' P^\nu, \tag{7}$$

and

$$\frac{dP^x}{dt} = \gamma P^\nu - \Gamma'' P^x, \tag{8}$$

where

$$\Gamma' = M\gamma + \Gamma^a + \Gamma^e_\nu, \quad \text{and} \tag{9}$$

$$\Gamma'' = \gamma + \Gamma^a + \Gamma^x \tag{10}$$

are the decay rates for states associated with states $|\nu\rangle$ and $|x\rangle$, respectively. As mentioned above, it is assumed that mode $|\nu\rangle$ dominates as an entrance VFR, and so direct excitation of the $|x\rangle$ modes is not included in Eq. (8).

Considered below is the possibility that $\Gamma^e_\nu \gg \Gamma^x$, modeling $|x\rangle$ as a gray or dark state (i.e., vibrational states in which the positron can remain for relatively long times without being ejected) as well as the limit $\Gamma^x \gg \Gamma^e_\nu$, modeling $|x\rangle$ as a multimode state with a subset of modes that can act as potent escape channels. Equations (7) and (8) neglect the coupling between the multimode vibrations $|x\rangle$. This follows from the assumption that all modes $|x\rangle$ couple to the positron continuum and to mode $|\nu\rangle$ with the same strengths per mode, Γ^x and γ, respectively. Thus they are treated identically as in Eq. (8).

The steady-state solutions of Eqs. (7) and (8) are

$$P^j = \frac{\Lambda_j}{\Gamma'\Gamma'' - M\gamma^2}, \tag{11}$$

where $j = \nu$ or x and

$$\Lambda_\nu = \Gamma''\Gamma^c \quad \text{and} \quad \Lambda_x = \gamma\Gamma^c. \tag{12}$$

The full time-dependent solutions for the populations $P^j(t)$ with the initial conditions $P^\nu = P^x = 0$ at $t = 0$ describe exponential relaxation to the steady state and involve two relaxation rates, ξ_+ and ξ_-,

$$P^j(t) = \frac{\Lambda_j}{\Gamma'\Gamma'' - M\gamma^2} \times \left[1 - e^{-\xi_- t} - \frac{(A_j - \xi_-)}{\xi_+ - \xi_-}(e^{-\xi_+ t} - e^{-\xi_- t})\right], \tag{13}$$

where $A_\nu = \Gamma' - M\gamma^2/\Gamma''$, $A_x = 0$, and

$$\xi_\pm = \tfrac{1}{2}\{\Gamma' + \Gamma'' \pm [(\Gamma' - \Gamma'')^2 + 4M\gamma^2]^{\frac{1}{2}}\}. \tag{14}$$

As an example, consider the case of one strongly coupled, fast-escape channel with $\gamma \gg \Gamma^x \gg \Gamma^e_\nu, \Gamma^a$. In this case,

$$P^\nu(t) \simeq P^x(t) \simeq \frac{\Gamma^c}{\Gamma^x}[1 - \exp(-\Gamma^x t/2)]. \tag{15}$$

During the transient buildup to saturation, states $|\nu\rangle$ and $|x\rangle$ are approximately equally populated (due to large γ), while only the population in state $|x\rangle$ escapes, and thus the characteristic time constant $\tau \sim 2/\Gamma^x$. For the complementary situation in which $\Gamma^x \gg \gamma \gg \Gamma^e_\nu, \Gamma^a$, Eq. (13) yields

$$P^\nu(t) \simeq \frac{\Gamma^c}{\gamma}(1 - e^{-\gamma t}) \gg P^x(t). \tag{16}$$

In this limit, the population P^ν is large compared to P^x, and $\tau \sim 1/\gamma$. These time-dependent solutions would be relevant, for example, in a fast (e.g., picosecond or less) optical pump-probe experiment where the start pulse was a photoinduced attachment [16]. However, in the experiments done to date, the P^j reach their saturated values on time scales $\lesssim 1/\Gamma^a$, much faster than those that can be measured experimentally. Thus, in the following, we consider only the steady-state values given by Eq. (11).

The annihilation rate Z_{eff} will be proportional to Γ^a multiplied by the probability that the positron is on the molecule. Using the steady-state P^j, the ensemble average Z_{eff} expected in experiment will be

$$Z_{\text{eff}} = \frac{\Gamma^a}{\Gamma^D}(P^\nu + MP^x) = \frac{\Gamma^a\Gamma^c}{\Gamma^D}\left(\frac{\Gamma'' + M\gamma}{\Gamma'\Gamma'' - M\gamma^2}\right), \tag{17}$$

where Γ^D is the Dirac annihilation rate defined in Eq. (1). Equation (17) is the principal governing equation in the model.

The capture rate Γ^c for mode ν in Eq. (7) can be calculated from the capture cross section [17]

$$\sigma_\nu(\varepsilon) = \frac{\pi\hbar^2}{k^2}\frac{\Gamma'\Gamma^e_\nu}{(\varepsilon + \varepsilon_b - \omega_\nu)^2 + (\hbar\Gamma'/2)^2}, \tag{18}$$

where ε is the incident positron energy, ω_ν is the energy of mode ν, and $k = mv/\hbar$, with m the positron mass and v its velocity. Anticipating measurements with a beam with finite energy spread $f(\varepsilon)$, the strength of the resonance is given by the convolution of σ_ν with $f(\varepsilon)$ (cf. Ref. [4]), resulting in

$$\overline{\sigma}_\nu \simeq \frac{2\pi^2\hbar\Gamma^e_\nu}{k^2\Delta E}, \tag{19}$$

where we have assumed that the spread in total energy of the positron beam is $\Delta E \gg \hbar\Gamma'$. The capture rate Γ^c is then given by [4]

$$\Gamma^c = n_m\overline{\sigma}_\nu v = \frac{\pi^2\hbar^3\Gamma^e_\nu n_m}{m^{3/2}\Delta E\sqrt{\varepsilon/2}} \equiv B\Gamma^e_\nu, \tag{20}$$

where, for use below, the second expression in Eq. (20) defines the dimensionless parameter B to display explicitly the dependence of Γ^c on Γ^e_ν.

The normalized annihilation rate Z_{eff} defined by Eq. (17) depends on four rates; Γ^e_ν, Γ^x, Γ^a, and γ and the number of multimodes M. To explore the dependence of Z_{eff} on the parameters that describe the positron-molecule coupling and vibrational dynamics, we define the dimensionless

enhancement and suppression factor β',

$$\beta' \equiv Z_{\rm eff}\left(\frac{B\Gamma^a}{\Gamma^D}\right)^{-1} = \Gamma^e_\nu\left(\frac{\Gamma'' + M\gamma}{\Gamma'\Gamma'' - M\gamma^2}\right). \tag{21}$$

While Eq. (21) is the central result of this paper, it can be rewritten in ways that clarify further the dependence of β' on the parameters of the model. Setting $\gamma = 0$ in Eq. (21) yields β' for a pure VFR

$$\beta'^{\rm VFR} = \frac{\Gamma^e_\nu}{\Gamma^e_\nu + \Gamma^a}. \tag{22}$$

Using this quantity, Eq. (21) can be rearranged to display explicitly the role of IVR, namely,

$$\beta' = \beta'^{\rm VFR}\frac{1 + M\delta}{1 + RM\delta}, \tag{23}$$

where the IVR coupling parameter δ is

$$\delta = \frac{\gamma}{\Gamma^x + \Gamma^a + \gamma}, \tag{24}$$

and the suppression and enhancement ratio R is

$$R = \frac{\Gamma^x + \Gamma^a}{\Gamma^e_\nu + \Gamma^a}. \tag{25}$$

As can be seen from Eq. (8), for the steady-state case considered here, the quantity $\delta = P^x/P^\nu$ represents the average population of state $|x\rangle$ relative to that in state $|\nu\rangle$. It spans the range $0 \leqslant \delta \leqslant 1$, modulating the strength of IVR. However, it is the parameter R alone that determines whether or not there is enhancement or suppression of β' relative to $\beta'^{\rm VFR}$. Whether R is greater or less than unity (i.e., suppression or enhancement, respectively) is seen to be independent of γ and determined solely by the ratio Γ^x/Γ^e_ν.

Equation (21) can also be rewritten in another insightful manner as

$$\beta' = \frac{\Gamma^e_\nu}{\langle\Gamma_\nu\rangle}, \tag{26}$$

with

$$\langle\Gamma_\nu\rangle = \frac{\Gamma^e_\nu + \Gamma^a + (\Gamma^x + \Gamma^a)M\delta}{1 + M\delta}. \tag{27}$$

Equation (26) indicates that β' is determined solely by the ratio of Γ^e_ν to the rate $\langle\Gamma_\nu\rangle$ of positron disappearance, including both annihilation and ejection from the molecule, averaged over state $|\nu\rangle$ and the $M\delta$ states $|x\rangle$.

To recapitulate, while all three forms of Eq. (21) are equivalent, Eqs. (23) and (26) provide additional insights into particular aspects of the underlying physics.

B. Limiting cases

Presented here is the scaling factor β' for simple but insightful special cases, focusing on suppression due to escape channels and enhancement due to M "gray" states. Since the parameter γ is poorly known, one limiting case chosen is an isolated VFR with $\gamma = 0$. The others, with one exception (case 2b below), are those where γ is assumed to be large compared to the other relevant parameters, which yields values of β' independent of γ. The results are summarized in Table I.

TABLE I. Limits of the dimensionless (enhancement or suppression) factor β' for $Z_{\rm eff}$ as defined in Eq. (21).

Effect / Case	Limit	β'
Isolated VFR		
$\gamma = 0$		
1a	$\Gamma^e_\nu \gg \Gamma^a$	1
1b	$\Gamma^a \gg \Gamma^e_\nu$	$\Gamma^e_\nu/\Gamma^a \ll 1$
Suppression		
$\Gamma^x, \gamma \gg \Gamma^e_\nu, \Gamma^a$		
2a	$(M+1)\gamma \gg \Gamma^x$	$(M+1)\Gamma^e_\nu/M\Gamma^x \ll 1$
2b	$\Gamma^x \gg (M+1)\gamma$	$\Gamma^e_\nu/M\gamma \ll 1$
Enhancement		
$\gamma \gg \Gamma^e_\nu \gg \Gamma^x, \Gamma^a$		
3a	$\Gamma^e_\nu \gg M\Gamma^x$ $\Gamma^x \gg \Gamma^a$	$(M+1) \geqslant 1$
3b	$M\Gamma^x \gg \Gamma^e_\nu$ $\Gamma^x \gg \Gamma^a$	$(M+1)\Gamma^e_\nu/M\Gamma^x \gg 1$
3c	$M \gg \Gamma^e_\nu/\Gamma^x$ $\Gamma^a \gg \Gamma^x$	$\Gamma^e_\nu/\Gamma^a \gg 1$

1. Isolated VFR

The parameter β' for an isolated fundamental vibration corresponds to $\gamma = 0$ and is given by Eq. (22). For $\Gamma^e_\nu \gg \Gamma^a$, $\beta' \to 1$ and the strength of the resonance is limited by Γ^a. If, on the other hand, $\Gamma^a \gg \Gamma^e_\nu$,

$$\beta' \to \frac{\Gamma^e_\nu}{\Gamma^a} \ll 1. \tag{28}$$

Equation (28) corresponds to the limit in which all positrons that attach to the molecule annihilate, namely,

$$Z_{\rm eff} = \frac{B\Gamma^a}{\Gamma^D}\beta' = \frac{\Gamma^c}{\Gamma^D}. \tag{29}$$

2. IVR suppression due to fast escape channels

Assuming $\Gamma^x, \gamma \gg \Gamma^e_\nu, \Gamma^a$,

$$\beta' \approx \Gamma^e_\nu\left(\frac{(M+1)\gamma + \Gamma^x}{M\gamma\Gamma^x}\right) \tag{30}$$

$$\to \frac{(M+1)\Gamma^e_\nu}{M\Gamma^x}, \quad \text{for} \quad (M+1)\gamma \gg \Gamma^x \tag{31}$$

$$\to \frac{\Gamma^e_\nu}{M\gamma}, \quad \text{for} \quad \Gamma^x \gg (M+1)\gamma. \tag{32}$$

In both limits of Eq. (30), $\beta' \ll \beta'^{\rm VFR}$ which results in suppression of the resonance. In the second limit, the suppression is limited by the mode coupling rate γ.

3. IVR enhancement due to M gray states

Assuming that $\gamma \gg \Gamma^e_\nu \gg \Gamma^x \gg \Gamma^a$, the expression for β' then becomes

$$\beta' \approx \left(\frac{M+1}{M\Gamma^x + \Gamma^e_\nu}\right)\Gamma^e_\nu \tag{33}$$

$$\to (M+1), \quad \text{for} \quad M\Gamma^x \ll \Gamma^e_\nu \tag{34}$$

$$\to \frac{(M+1)\Gamma^e_\nu}{M\Gamma^x}, \quad \text{for} \quad M\Gamma^x \gg \Gamma^e_\nu. \tag{35}$$

TABLE II. Comparison of Z_{eff} measurements (β' obs.) for selected molecules, chosen to correspond to the limiting cases in Table I, with the predictions of the model (β' est.) that are made using the limiting expressions in the table. See text for details. Rates Γ_ν^e, Γ^x, and Γ^a are given in units of gigahertz. $\langle xx \rangle$ notation indicates that the value xx is an estimated average. Superscripts on the Γ_ν^e values indicate the source of the IR absorption values used in calculating the rates: (a) measured values taken from Ref. [18] and (b) calculated values in the B3LYP ultrafine density functional theory, using a 6-31G* basis set, obtained from Ref. [19]. The absence of a predicted value of β' for case 2b is discussed in the text.

Case	Type	Limit	Example	Γ_ν^e	Γ^x	Γ^a	β' est.	β' obs.
1a	Isolated VFR	$\Gamma_\nu^e \gg \Gamma^a$	CH_3Cl / CCl str	100^a	n.a.	0.21	1.0	1.0
1b		$\Gamma_\nu^e < \Gamma^a$	$C_2H_2Cl_2$ / CCl rock	0.06^b	n.a.	0.3	0.2	n.a.
2a	Suppression	$(M+1)\gamma > \Gamma^x$	$CDCl_3$ / CD str	0.6^a	$\langle 1{,}000 \rangle$	0.3	0.001	0 (0.1)
2b		$\Gamma^x > (M+1)\gamma$	$CHCl_3$ / CH str	1.8^a	$\langle 1{,}900 \rangle$	0.3	n.a.	0.4 (0.1)
3a	Enhancement	$\Gamma_\nu^e \gg M\Gamma^x$; $\Gamma^x > \Gamma^a$	C_3H_6O / C=O str	320^b	$\langle 4.4 \rangle$	0.5	11	7.9 (0.5)
3b		$M\Gamma^x \gg \Gamma_\nu^e \gg \Gamma^x$; $\Gamma^x > \Gamma^a$	C_8H_{18} / CH str	$\langle 310 \rangle^b$	$\langle 1.5 \rangle$	0.5	210	210 (8)
3c		$M\Gamma^x \gg \Gamma_\nu^e$; $\Gamma^a > \Gamma^x$	$C_{12}H_{26}$ / CH str	$\langle 150 \rangle^b$	<0.6	0.6	250	740 (60)

As indicated by Eqs. (34) and (35), the VFR is IVR-enhanced and grows proportional to the number of gray states M but then saturates at the value given by Eq. (35) when $M\Gamma^x \geqslant \Gamma_\nu^e$. Finally, there is another limit, namely, $\gamma \gg \Gamma_\nu^e \gg \Gamma^a \gg \Gamma^x$, but $M \gg 1$, so that $M\Gamma^x \gg \Gamma_\nu^e$, for which

$$\beta' \to \frac{\Gamma_\nu^e}{\Gamma^a} \gg 1. \tag{36}$$

This limit also describes saturation, where all positrons that attach to the molecule annihilate—the same limit as described in Eqs. (28) and (29) above. In particular, $Z_{\text{eff}} = B(\Gamma^a/\Gamma^D)\beta' = \Gamma^c/\Gamma^D$.

III. COMPARISON WITH SELECTED EXPERIMENTAL OBSERVATIONS

Given that the simple model presented here aims to describe a complex process using restrictive assumptions and a small number of parameters (i.e., assuming only one type of multimode state $|x\rangle$ with one escape rate Γ^x and one mode-coupling rate γ), it is unrealistic to expect that systematic and detailed comparisons with experimental measurements for resonant Z_{eff} magnitudes can be made. Thus discussed here are selected examples that approximate the limiting cases discussed in Sec. II and summarized in Table I. The results of these comparisons are summarized in Table II.

In these comparisons, the broad background contributions to the experimental Z_{eff} spectra due to the direct annihilation $Z_{\text{eff}}^{\text{dir}}$ and the SMRA contribution $Z_{\text{eff}}^{\text{SMRA}}$ [13] are first subtracted [11], then values of β' are obtained from a fit to the resulting Z_{eff} data of the form

$$Z_{\text{eff}}^{\text{fit}} = \sum_\nu \beta'_\nu \left(\frac{B_\nu \Gamma^a}{\Gamma^D} \right), \tag{37}$$

where B_ν is the value of the parameter B at resonance ν. The energy-resolved Z_{eff} spectra as a function of incident positron energy are used for these fits, including the energy distribution of the incident positron beam. For further details regarding the fitting, including the background subtractions, see Ref. [11].

It should be noted that the parameter β' used here differs from the parameter β in Ref. [11]. The normalization of β' explicitly includes the complete dependence upon Γ_ν^e and Γ^a, so as to be able to distinguish cases 1a and 1b and recover the limit that Z_{eff} is vanishingly small when $\Gamma_\nu^e \ll \Gamma^a$.

Presented below are examples selected to match (or at least best approximate) the limits in Table I. The molecules and specific resonant modes were also chosen with experimental considerations in mind, namely, ones where the resonance is relatively isolated, the relevant multimode states can be identified, and the coupling of both the primary resonance and the multimodes to the positron continuum can be estimated from infrared data. The elastic rates are calculated from the absolute integrated IR intensities using Eq. (5) [10]. Since this assumes that the interaction of the incident positron with the molecule is due solely to dipole coupling, it provides lower bounds for the elastic rates.

As mentioned above, among the uncertainties in these comparisons is the assumed magnitude of γ. Generally, theoretical calculations of this parameter relevant to the molecules discussed here are unavailable. Further, there is evidence that mode coupling and IVR occurs for positron VFR when the multimode spacing is larger (level density smaller) than in the case of photoinduced IVR (i.e., which is the major source of γ data) [4]. This trend is also seen in the examples given below: IVR from low-order multimodes requires coupling to modes with spacings up to several millielectronvolts apart, which is considerably greater than that observed in the photon case. This difference is not presently understood.

The majority of the data to be presented here for annihilation rates for molecules resolved as a function of incident positron energy have been published previously. The experimental apparatus and procedures for these measurements are discussed in detail elsewhere [4]. To orient the reader, positrons from a radioactive source and solid neon moderator are cooled in a Penning-Malmberg buffer-gas trap, then released to produce a pulsed beam with a parallel energy spread of ~25 meV. The component of beam energy perpendicular to the axial magnetic field is a Maxwellian distribution at the same temperature as the buffer gas (i.e., 25 meV). To account for this energy, 12 meV is added to the measured parallel energy to yield the actual, mean positron energy [4]. Annihilation measurements are made in a gas cell downstream of the trap. Spectra are measured by the detection of single 511-keV annihilation γ rays. Further details are discussed in Ref. [4].

1. Isolated VFR

1a. An example of an isolated resonance where $\Gamma_\nu^e \gg \Gamma^a$ is the ν_3 C-Cl stretch mode of methyl chloride (CH_3Cl, $\varepsilon_b = 19$ meV, $\Gamma^a = 0.21$ GHz), for which $\omega_\nu = 91$ meV and $\Gamma_\nu^e = 100$ GHz [4]. Due to the relatively low frequency of this vibration, no enhancement or decay channels are available to modify the magnitude of the VFR.

1b. An example of a resonance where $\Gamma_\nu^e \ll \Gamma^a$ is the ν_{10} C-Cl_2 rock mode of 1,1-dichloroethylene (1,1-DCE, $C_2H_2Cl_2$, $\varepsilon_b = 33$ meV, $\Gamma^a = 0.3$ GHz), with $\omega_\nu = 46$ meV and $\Gamma_\nu^e = 0.06$ GHz. Using Eq. (28), β' for this mode is estimated to be 0.2. Unfortunately, the relatively low energy of the resonance and the proximity of other modes prevents measurement of β' for this molecule [20].

2. IVR suppression

2a. Suppression for strong mode coupling corresponds to the limit $\Gamma^x, \gamma \gg \Gamma_\nu^e, \Gamma^a$; and $(M+1)\gamma \gg \Gamma^x$. An example of this case is the ν_1 C-D stretch mode of deuterated chloroform ($CDCl_3$, $\varepsilon_b = 43$ meV) at $\omega_\nu = 281$ meV [11]. This example is illustrated in Fig. 2(a), with the region of the suppressed VFR shown in expanded detail in the inset. This mode is, to within experimental uncertainty, completely suppressed, namely, $\beta' = 0 \pm 0.1$. For this case, Γ_ν^e is ~ 0.6 GHz, which is comparable to $\Gamma^a = 0.3$ GHz. In this molecule, combination modes that include the C-Cl stretch mode can act as effective escape channels. Considering that there are ten three-mode combinations within 8 meV of the entrance channel [11], the prediction of Eq. (31) is $\beta' = 0.001$.

2b. Suppression with weaker mode coupling than case 2a is the limit $\Gamma^x, \gamma \gg \Gamma_\nu^e, \Gamma^a$, as in the case 2a, but with $(M+1)\gamma \ll \Gamma^x$. The smaller value of γ limits the multimode coupling and hence reduces the suppression. In this case, β' is inversely proportional to γ. While we do not find an example that fits exactly the case 2b limit, a closely related example is the ν_1 C-H stretch mode in chloroform ($CHCl_3$, $\varepsilon_b = 40$ meV) at $\omega_\nu = 376$ meV [11], illustrated in Fig. 2(b), with an expanded view of the region of interest in the inset. For this mode, $\Gamma_\nu^e = 1.8$ GHz and $\beta' = 0.4 \pm 0.1$.

Examination of the multimodes in close proximity to mode ν indicates that the lowest order is four-mode combinations. Of the 31 modes within 8 meV of the entrance channel, 25 contain the strongly IR active asymmetric C-Cl stretch mode [11]. If the expression for case 2a were used, this would result in $\beta' = 0.001$, in striking disagreement with the observed value. This leads us to consider case 2b. In this case, the predicted value of β' will depend explicitly on γ. Since no estimate of γ is available for the positron experiments, the estimate of β' is absent in Table II.

However, in this case, the full expression in Eq. (21) and the measured value of β' can be used to estimate γ, yielding $\gamma = 0.08$ GHz. In making this estimate, use of Eq. (21) is required, due to the fact that $\gamma < \Gamma_\nu^e, \Gamma^a$, so that the simple case 2b limit described in Table I is invalid.

The difference in IVR suppression between deuterated chloroform and chloroform is qualitatively consistent with the relaxation rates measured previously in weakly interacting solutes using optical techniques. The characteristic time constant is approximately a factor of 10 longer for the C-H stretch mode of chloroform [21] than the C-D stretch mode of chloroform-d [22].

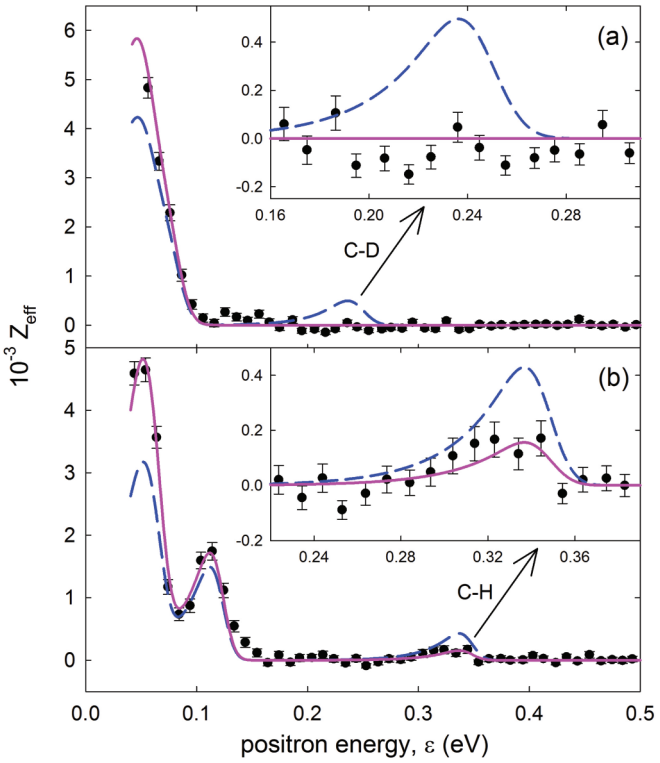

FIG. 2. (Color online) Examples of suppressed VFRs for (a) chloroform-d ($CDCl_3$, $\varepsilon_b = 43$ meV) and (b) chloroform ($CHCl_3$, $\varepsilon_b = 40$ meV): (•) experimental data, (– –) unscaled VFR model, and (—) model fit. Insets highlight the suppression of (a) the C-D stretch mode in $CDCl_3$, and (b) the C-H stretch mode in $CHCl_3$. The spectra shown are background-subtracted to eliminate contributions due to direct annihilation and SMRA.

3. IVR enhancement

Enhancement occurs when the entrance vibration couples to multimodes that have smaller escape rates.

3a. This case describes the situation in which $\Gamma_\nu^e \gg M\Gamma^x$. An example is the C=O stretch mode of propanal (C_3H_6O, $\varepsilon_b = 116$ meV), where $\omega_\nu = 218$ meV and $\Gamma_\nu^e = 320$ GHz [23]. The spectrum is illustrated in Fig. 3(a), where the VFR due to the C=O stretch mode is located at ~100 meV. Any model that neglects the coupling of the C=O stretch resonance to other vibrations will likely seriously underestimate Z_{eff} near $\varepsilon \approx 0.1$ eV. Fitting the resonance yields $\beta' = 7.9 \pm 0.5$. The number of near-resonant multimodes containing just two vibrations in a range of ± 8 meV about the C=O stretch vibration is 10. In this case, Eq. (34) yields the estimate $\beta' = 11$, which is in good agreement with the observation.

3b. This is again a case of enhancement, but one in which the ratio Γ_ν^e/M is smaller: $M\Gamma^x \gg \Gamma_\nu^e \gg \Gamma^x$. In this case, β' scales differently, saturating for $M \gg 1$ at $\beta' \sim \Gamma_\nu^e/\Gamma^x$. The enhancement of the C-H stretch modes in moderate to large alkanes appear to fit this picture. This is illustrated in Fig. 3(b) for octane (C_8H_{18}, $\varepsilon_b = 125$ meV) [24], where the resonant feature associated with the C-H stretch vibrations, observed at ~240 meV, is seen to be enhanced significantly above the

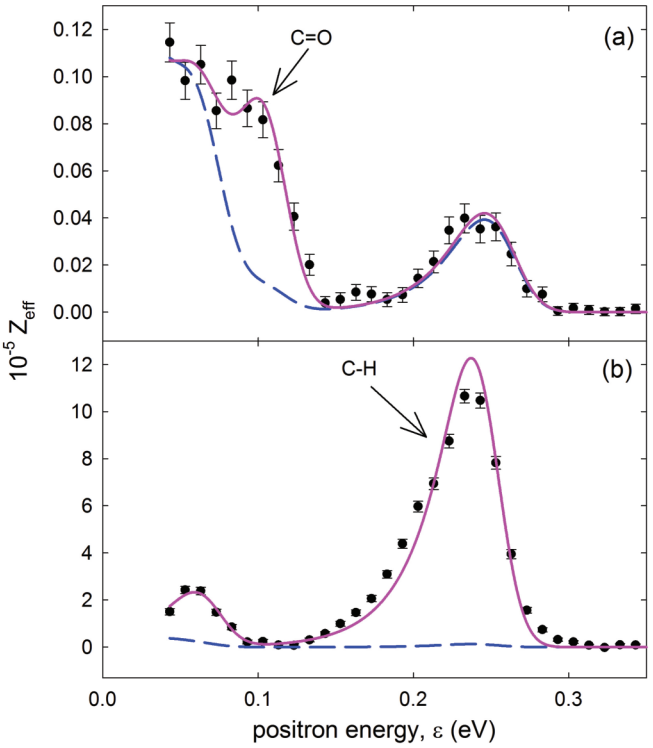

FIG. 3. (Color online) Examples of enhanced VFRs: (a) the C=O stretch mode in propanal (C_3H_6O, $\varepsilon_b = 115$ meV) and (b) the C-H stretch mode in octane (C_8H_{18}, $\varepsilon_b = 125$ meV): (•) experimental data, (– –) unscaled VFR model, and (—) model fit. The spectra shown are background-subtracted to eliminate contributions due to direct annihilation and SMRA.

magnitude predicted by the VFR model. In octane, nine of the 18 C-H stretch modes are infrared active, and the average elastic rate Γ^e_ν for these modes is approximately 310 GHz. The average escape rate Γ^x of the two- and three-mode combinations near resonant with the C-H stretch vibrations, comprised primarily of C-H bend mode combinations, is approximately 1.5 GHz. Thus the expected enhancement of $\beta' \simeq 202$ is in reasonable agreement with the observed enhancement of ∼210 per IR-active C-H stretch mode.

3c. This third limit of enhancement relates to the situation in which the $|x\rangle$ multimodes have very small ejection rates, namely $\Gamma^x \ll \Gamma^a$, but where $M\Gamma^x > \Gamma^e_\nu$. This limit likely describes, for example, annihilation in the largest alkanes studied to date, where ε_b is larger than the energies of most fundamental vibrations, closing off the available escape channels. Once an entrance VFR couples to lower energy modes, the positron is effectively trapped on the molecule, and the rate of annihilation is the capture rate.

A possible example of this is the C-H stretch modes of dodecane ($C_{12}H_{26}$, $\varepsilon_b = 209$ meV), where $\beta' \sim 740$ per IR-active mode [4]. As limited information is available regarding the vibrational modes of dodecane, we assume the dipole coupling is similar to that predicted for octane. Taking into account the differences in binding energy, $\Gamma^e_\nu \sim 150$ GHz for dodecane. Given that all fundamentals less energetic than the C-H stretch modes cannot individually eject the positron due to the ε_b value of 220 meV, Γ^x is likely to be less than Γ^a, which is 0.6 GHz, while the number of multimodes M is very large. The predicted enhancement, $\beta' = 233$, is only in qualitative agreement with that observed (i.e., 233 as compared with 744). It is also not presently clear that $M\Gamma^x > \Gamma^a$, as Γ^x must involve deexcitation of two or more vibrational modes.

IV. CONCLUDING REMARKS

Annihilation on molecules in the range of incident positron energies corresponding to those of the vibrational modes is typically dominated by vibrational Feshbach resonances. While there is a theory of VFR for isolated modes in simple molecules, the spectra from most molecules appear to exhibit departures from this theory, and there is considerable evidence that these departures involve coupling to other vibrations.

Presented here is a simple model describing the effects of this IVR on the magnitudes of the VFRs. In the model, the entrance VFR is coupled to M identical multimode states. Such multimodes have been observed previously as broad features in resonant annihilation spectra (i.e., SMRA [13]). Here it is shown that they can have an important effect on VFR involving fundamental vibrations; when the coupling is strong, the VFR amplitude can be modified significantly. Either suppression or enhancement can result, depending upon the coupling to the positron continuum of the fundamentals comprising the multimode states.

Due to the sweeping nature of the approximations made here, systematic and quantitative comparison with experiment is unrealistic. While a more realistic model hinges on understanding in greater detail the intricacies of IVR-related mode coupling, the present model does provide insight into the general features of the expected behavior. In particular, it highlights the key role played by the strength of the mode-coupling rate γ relative to the elastic escape rates of the entrance state and multimodes in determining the amplitudes of VFR. Estimates for the elastic rates Γ^e_ν and Γ^x can be made using the dipole approximation, and the rate of annihilation while the positron is on the molecule Γ^a can be estimated to reasonable accuracy. However, as discussed in Sec. III above, a key impediment to further progress at present is systematic knowledge of γ.

ACKNOWLEDGMENTS

We thank G. F. Gribakin for helpful discussion and suggestions and E. L. Sibert III for helpful discussions. We also wish to thank E. A. Jerzewski for his expert technical assistance. This work is supported by US NSF Grant No. PHY 10-68023.

[1] *Principles and Practice of Positron Emission Tomography*, edited by R. L. Wahl (Lippincott Williams & Wilkins, Philadelphia, PA, 2002).

[2] D. W. Gidley, H.-G. Peng, and R. S. Vallery, Annu. Rev. Mater. Sci. **36**, 49 (2006).

[3] N. Guessoum, P. Jean, and W. Gillard, Mon. Not. R. Astron. Soc. **402**, 1171 (2010).

[4] G. F. Gribakin, J. A. Young, and C. M. Surko, Rev. Mod. Phys. **82**, 2557 (2010).
[5] J. R. Danielson, J. A. Young, and C. M. Surko, J. Phys. B: At. Mol. Opt. Phys. **42**, 235203 (2009).
[6] J. R. Danielson, J. J. Gosselin, and C. M. Surko, Phys. Rev. Lett. **104**, 233201 (2010).
[7] M. Tachikawa, R. J. Buenker, and M. Kimura, J. Chem. Phys. **119**, 5005 (2003).
[8] M. Tachikawa, Y. Kita, and R. N. Buenker, Phys. Chem. Chem. Phys. **13**, 2701 (2011).
[9] K. Strasburger, Struct. Chem. **15**, 415 (2004).
[10] G. F. Gribakin and C. M. R. Lee, Phys. Rev. Lett. **97**, 193201 (2006).
[11] A. C. L. Jones, J. R. Danielson, M. R. Natisin, and C. M. Surko, Phys. Rev. Lett. **110**, 223201 (2013).
[12] G. Gribakin and P. Gill, Nucl. Instrum. Methods Phys. Res., Sect. B **221**, 30 (2004).
[13] A. C. L. Jones, J. R. Danielson, M. R. Natisin, C. M. Surko, and G. F. Gribakin, Phys. Rev. Lett. **108**, 093201 (2012).
[14] D. J. Nesbitt and R. W. Field, J. Phys. Chem. **100**, 12735 (1996).
[15] S. Twagirayezu, X. Wang, D. S. Perry, J. L. Neill, M. T. Muckle, B. H. Pate, and L.-H. Xu, J. Phys. Chem. A **115**, 9748 (2011).
[16] C. M. Surko, J. R. Danielson, G. F. Gribakin, and R. E. Continetti, New J. Phys. **14**, 065004 (2012).
[17] L. D. Landau and E. M. Lifshitz, *Quantum Mechanics: Non-Relativistic Theory Vol. 3*, 3rd ed. (Permagon Press, New York, 1977).
[18] D. M. Bishop and L. M. Cheung, J. Phys. Chem. Ref. Data **11**, 119 (1982).
[19] NIST computational chemistry comparison and benchmark database, http://cccbdb.nist.gov/
[20] A. C. L. Jones, M. R. Natisin, J. R. Danielson, and C. M. Surko (unpublished).
[21] H. J. Bakker, J. Chem. Phys. **98**, 8496 (1993).
[22] K. Gündoğdu, M. W. Nydegger, J. N. Bandaria, S. E. Hill, and C. M. Cheatum, J. Chem. Phys. **125**, 174503 (2006).
[23] J. R. Danielson, A. C. L. Jones, J. J. Gosselin, M. R. Natisin, and C. M. Surko, Phys. Rev. A **85**, 022709 (2012).
[24] L. D. Barnes, S. J. Gilbert, and C. M. Surko, Phys. Rev. A **67**, 032706 (2003).